ISSN 0018-1439, High Energy Chemistry, 2022, Vol. 56, No. 1, pp. 38–41. © Pleiades Publishing, Ltd., 2022.
Russian Text © The Author(s), 2022, published in Khimiya Vysokikh Energii, 2022, Vol. 56, No. 1, pp. 45–49.

PHOTOCATALYSIS

Inorganic Ruthenium Catalyst for Photoinduced Oxidation of Water in Artificial Photosynthesis

V. Yu. Il'yashchenko[a, b], **Z. M. Dzhabieva**[b], **T. A. Savinykh**[b], **L. V. Avdeeva**[b], **and T. S. Dzhabiev**[b, *]
[a] *Moscow State University, Moscow, 119991 Russia*
[b] *Institute for Problems of Chemical Physics, Russian Academy of Sciences, Chernogolovka, Moscow oblast, 142432 Russia*
**e-mail: dzhabiev@icp.ac.ru*

Received July 26, 2021; revised August 23, 2021; accepted August 28, 2021

Abstract—The reaction of photocatalytic oxidation of water with potassium persulfate in the presence of the photosensitizer $bpy_3RuCl_2·6H_2O$ and the ruthenium nitride complex $Li_3[Ru_2(\mu\text{-}N)Cl_8·2H_2O]$ has been studied. It has been found by kinetic and electrospray-ionization mass spectrometry methods that the catalyst for the process is the tetraruthenium complex $Ru_4N_2O_5^+$ with a molecular weight of 512.28 amu. The efficiency of the catalytic system (a turnover number of TON = 360, a O_2 quantum yield of $\Phi = 0.51$) is higher than that of its oxygen analogue $Li_4[Ru_2OCl_{10}·2H_2O]$ (TON = 240 and $\Phi = 0.2$).

Keywords: artificial photosynthesis, photocatalysis, water oxidation, O_2 quantum yield, tetraruthenium complex

DOI: 10.1134/S0018143922010064

In connection with environmental problems, the 21st century will become that of transition from hydrocarbon energy to other types of energy carriers; therefore, the search for new alternative energy sources begins to be very important. Solar energy (SE) is such an alternative. One of the most promising ways of converting SE is its biomimetic utilization, based on the possibility of photoinduced splitting of water into oxygen and hydrogen, i.e. on artificial photosynthesis (APS). Research in this area all over the world is going on purposefully and widely. The most difficult catalytic step of artificial photosynthesis is the formation of multielectron products of water oxidation by one-electron oxidants. One-electron oxidizing (and reducing) agents are formed in the photochemical step of photosynthesis after absorption of light quanta. In natural photosynthesis, radical cations $P680^+$ act as an oxidant of this type and the catalyst is a manganese cofactor (Mn_4CaO_5), in the coordination sphere of which an O_2 molecule is formed according to the reaction: $4P680^+ + 2H_2O = 4P680 + O_2 + 4H^+$. In artificial photosynthesis, clusters of other transition metals, including ruthenium, are used for this purpose.

Recent studies have shown that polynuclear ruthenium complexes are of interest as promising high-performance catalysts for water oxidation in artificial photosynthesis with the aim to create photocatalytic converters of solar energy into chemical fuel energy in the future [1–5]. However, these catalysts are far from perfect because they do not have sufficient activity. In addition, there are a number of problems associated with their use in model systems. Most of them contain organic ligands, which are oxidized more readily than water, and labile Ru–O–Ru bonds leading to catalyst deactivation [6–10]. It was found that the replacement of the oxygen bridge between the Ru nuclei in the complex (Ru–O 1.86 Å) by the nitrogen bridge (Ru–N 1.72 Å), as well as the use in the synthesis of inorganic ligands and various countercations (Li^+, K^+, Rb^+, Cs^+), whose substitution can change the stoichiometric composition of the complex, has a decisive effect on the stability and activity of water oxidation catalysts [11–15].

This paper presents the results of a study of the photocatalytic oxidation of water with potassium persulfate in the presence of the photosensitizer $bpy_3RuCl_2·6H_2O$ and the binuclear ruthenium nitride complex with lithium countercations $Li_3[Ru_2(\mu\text{-}N)Cl_8·2H_2O]$ (**1**).

EXPERIMENTAL

All operations for the synthesis of the $Li_3[Ru_2(\mu\text{-}N)Cl_8·2H_2O]$ complex were carried out in air. The chemicals used in this work were commercial materials (Fluka). The synthesis of the complex and its X-ray analysis are described in [15]. IR spectra were recorded on a Bruker INVENIO R Fourier-transform IR spectrometer (Germany) in the range of 6000–80 cm^{-1}; a sample for analysis was prepared in the

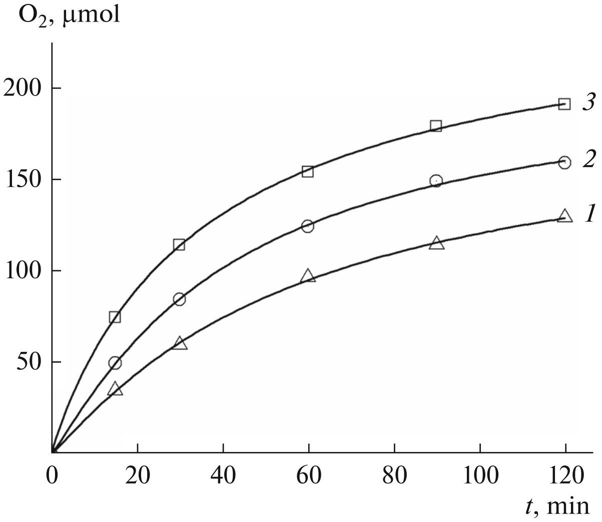

Fig. 1. Kinetics of photocatalytic formation of O_2 at different $Li_3[Ru_2NCl_8{\cdot}2H_2O]$ concentrations of (*1*) 3×10^{-5}, (*2*) 6×10^{-5}, (3) and 1×10^{-4} mol/L. Conditions: DRSh-1000 lamp, interference filter λ = 450 nm, $d_{reactor}$ = 3.7 cm, V = 25 mL, 3 M HCl, $[bpy_3RuCl_2]$ = 1.0×10^{-3} mol/L, $[K_2S_2O_8]$ = $8\ 5 \times 10^{-2}$ mol/L.

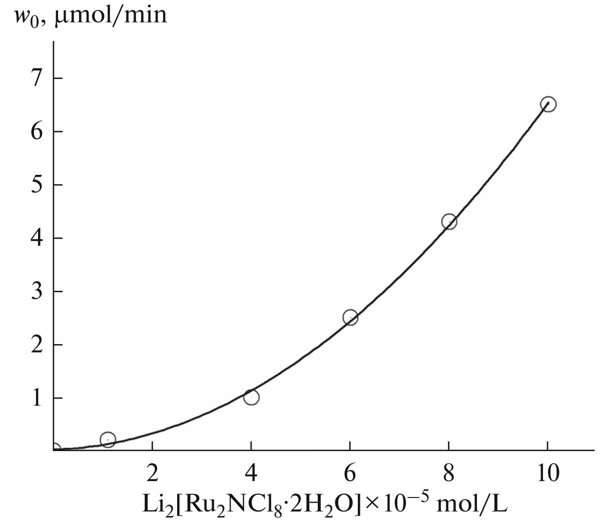

Fig. 2. Dependence of the initial rate of O_2 formation (w_0) on the $Li_3[Ru_2NCl_8{\cdot}2H_2O]$ concentration.

form of a KBr disk. The composition and structure of the in situ formed tetranuclear catalyst for water photooxidation were determined using electrospray ionization (ESI) mass spectrometry. Its mass spectrum was obtained on a Shimadzu LCM-2020 liquid chromatograph—mass spectrometer (Japan).

Oxygen formation rate curves were measured using a glass vacuum unit. A DRSh-1000 ultrahigh-pressure mercury lamp was used as a light source. The desired wavelength was selected using an interference filter with λ = 450 nm. The light intensity (I_0) was determined with a ferrioxalate actinometer under the same conditions as those for the photolysis of the test samples (I_0 (450 nm) = 1.9×10^{-7} einstein/s) [16]. The oxygen quantum yield (Φ) was determined according to the relation $\Phi = W_0/I_0$, where W_0 is the initial rate of oxygen formation. Before irradiation, solutions of bpy_3RuCl_2, $K_2S_2O_8$, and complex **1** were loaded into a fused-quartz reactor protected from light with aluminum foil, quickly purged with high-purity nitrogen, and degassed in a vacuum. After each irradiation, the amount of O_2 formed was determined using a calibrated manometer. Gaseous products of the reaction were collected in a mass spectrometric ampoule and analyzed on a MI-1201 mass spectrometer (Selmi, Russia).

RESULTS AND DISCUSSION

In dilute aqueous solutions, Cl^- ions in complex **1** are partially replaced by H_2O and OH groups, but the Ru—N—Ru moiety is retained, as indicated by the frequency of its stretching vibrations ν^{as} = 1075 cm^{-1} in the IR spectrum. Complex **1** is stable in acidic solutions. The catalytic oxidation of water by cerium ammonium nitrate $(NH_4)_2Ce(NO_3)_6$ in the presence of **1** occurs via the four-electron mechanism according to reaction (I) [15]:

$$4Ce^{IV} + 2H_2O = 4Ce^{III} + O_2 + 4H^+. \qquad (1)$$

The O_2 formation kinetics was studied as a function of the concentration of complex **1**, the oxidizing agent $K_2S_2O_8$, and the photosensitizer $bpy_3RuCl_2{\cdot}6H_2O$. Figure 1 shows the rate curves of O_2 formation at different concentrations of complex **1**. They have the usual form with a maximum rate at the beginning, which decreases with time. This is obviously due to the consumption of the "sacrificial" electron scavenger $S_2O_8^{2-}$.

The plot of the initial rate of the process w_0 versus the concentration of complex **1** is an S-shaped curve, which is well described by the parabolic law at low concentrations (from 1.1×10^{-5} to 10^{-4} mol/L) (Fig. 2). This indicates that the catalytically active species is formed from two binuclear nitride complexes **1** and is a tetranuclear ruthenium cluster. The composition of the tetranuclear complex of ruthenium was determined by ESI mass spectrometry. In the mass spectrum shown in Fig. 3 for the products of the photocatalytic oxidation of water, the isotopic distribution has the highest peak at m/z 512.28, which corresponds to the tetraruthenium dinitride cation in agreement with the calculated value (m/z 512.30). The efficiency of the photocatalytic system as a function of the concentration of complex **1** is shown in Fig. 4, from which it can be seen that the maximum

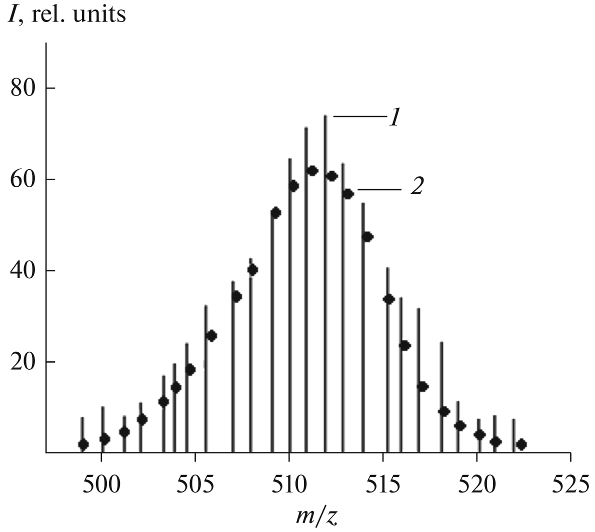

Fig. 3. ESI mass spectrum of the catalyst for the reaction of water oxidation in a mixture of $CH_3CN : H_2O : HCOOH = 29 : 70 : 1$, (*1*—experiment; *2*—calculation).

catalyst turnover number (TON) is 360 at [1] = 1.1 × 10^{-5} mol/L (Fig. 4a) and the quantum yield (Φ) of O_2 is 0.51 at [1] = 1.1 × 10^{-4} mol/L (Fig. 4b).

The initial rate of O_2 formation with an increase in the concentration of the "sacrificial" oxidant $K_2S_2O_8$ has the form of an S-shaped curve as well, which also indicates the consumption of two scavengers in the course of the reaction. After passing through the inflection point of the curve (5 × 10^{-2} mol/L), the rate sharply decreases and goes to an almost constant value. Table 1 shows the oxygen yield (*Q*) for 2 h of reaction, the catalyst turnover number (TON), and the O_2 quantum yield (Φ) depending on the $K_2S_2O_8$ concentration. The dependence of the initial rate of H_2O photooxidation on the concentration of the photosensitizer is shown in Fig. 5. It is a nonmonotonic curve with a maximum at $[bpy_3RuCl_2{\cdot}6H_2O] = 2 \times 10^{-3}$ mol/L. In this case, the concentration self-quenching of the photosensitizer is explained by the transfer of excitation energy not to the monomeric molecule but to the nonfluorescent dimer $(bpy_3RuCl_2^{2+})_2$, which dissipates the excitation energy into heat [17].

Table 1. Dependence of the O_2 yield (Q_{O_2}), catalyst turnover number (TON) for 2 h, and the quantum yield (Φ_{O_2}) on the $K_2S_2O_8$ concentration

$[K_2S_2O_8] \times 10^{-2}$ mol/L	Q_{O_2}	TON	Φ_{O_2}
2.5	0.36	45	0.17
5.0	0.31	77	0.34
10.0	0.17	87	0.64

TON = O_2 yield for 2 h/ [1]; Q_{O_2} = O_2 yield for 2 h/$K_2S_2O_8$/2; $\Phi_{O_2} = w_0/I_0$.

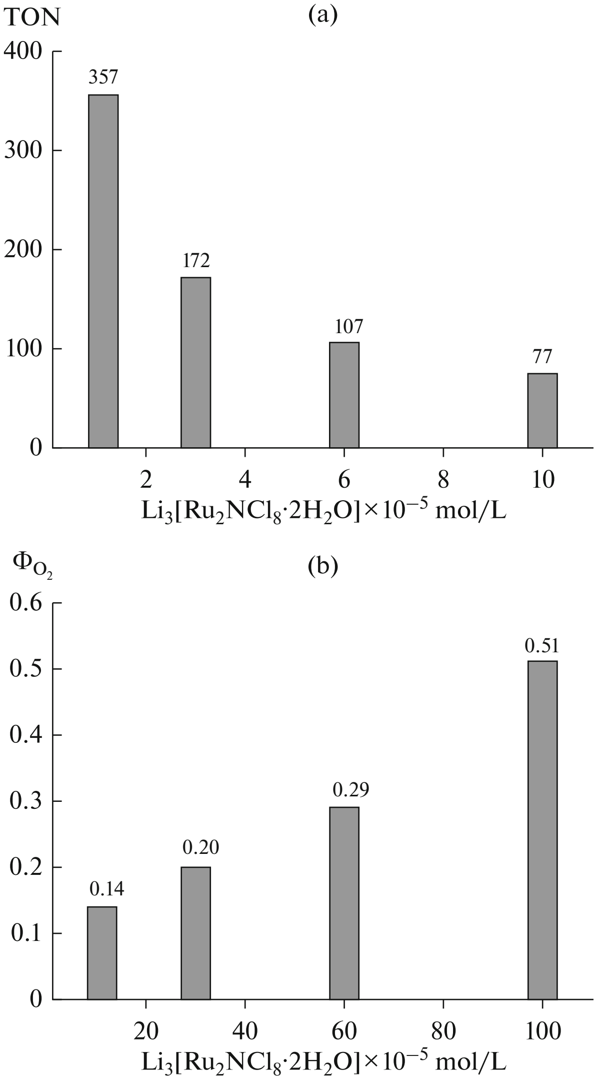

Fig. 4. Dependence of (a) the catalyst turnover number (TON) and (b) the quantum yield of O_2 (Φ) on the $Li_3[Ru_2NCl_8{\cdot}2H_2O]$ concentration.

Photogeneration of one-electron oxidants can be represented by reactions (2)–(4):

$$bpy_3RuCl_2^{2+} + h\nu \rightarrow bpy_3RuCl_2^{2+*}, \quad (2)$$

$$bpy_3RuCl_2^{2+*} + S_2O_8^{2-} = bpy_3RuCl_2^{3+} + SO_4^{-\bullet} + SO_4^{2-}, \quad (3)$$

$$bpy_3RuCl_2^{2+} + SO_4^{-\bullet} = bpy_3RuCl_2^{3+} + SO_4^{2-}. \quad (4)$$

Thus, upon absorption of a quantum of light, two $bpy_3RuCl_2^{2+}$ molecules are oxidized into two molecules of $bpy_3RuCl_2^{3+}$, and the persulfate anion

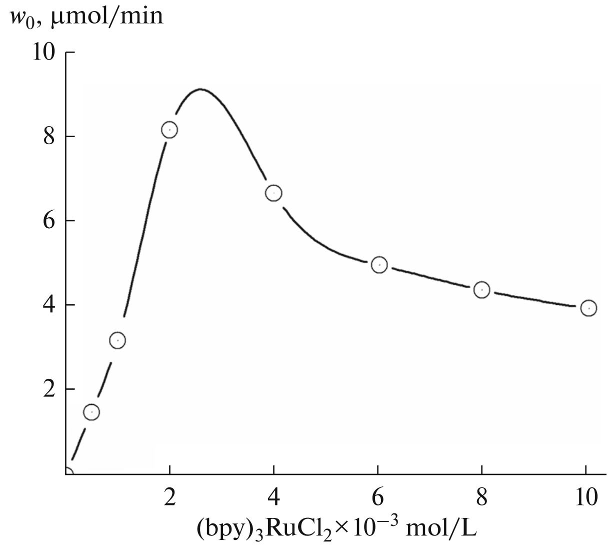

Fig. 5. Change in the initial rate of the process (w_0) with the photosensitizer (bpy_3RuCl_2) concentration at $[Li_3[Ru_2NCl_8{\cdot}2H_2O]] = 1 \times 10^{-4}$ mol/L and $[K_2S_2O_8] = 5 \times 10^{-2}$ mol/L.

is reduced into two sulfate anions according to reaction (5):

$$2bpy_3RuCl_2^{2+*} + S_2O_8^{2-} = 2bpy_3RuCl_2^{3+} + 2SO_4^{2-}. \quad (5)$$

Table 2 shows the activity of the catalytic system depending on the photosensitizer concentration.

To summarize, in the photocatalytic oxidation of water with potassium persulfate, the catalyst is the tetranuclear dinitride complex of ruthenium, which is formed as a result of dimerization of two initial binuclear complexes **1**. The efficiency of the catalytic system (TON = 360 and $\Phi = 0.51$) is higher than that of its oxygen analogue $Li_4[Ru_2OCl_{10}{\cdot}2H_2O]$ (TON = 250 and $\Phi = 0.2$).

FUNDING

The work was carried out within the framework of the State Assignment no. AAAA-A19-119071190045-0 using equipment of the Shared-Use Analytical Center at the Institute for Problems of Chemical Physics, Russian Academy of Sciences.

Table 2. Dependence of the O_2 yield (Q_{O_2}), the turnover number (TON) for 2 h of reaction, and the quantum yield (Φ_{O_2}) on $[bpy_3RuCl_2]$

$[bpy_3RuCl_2] \times 10^{-3}$ mol/L	Q_{O_2}	TON	Φ_{O_2}
0.5	0.125	32	0.13
1.0	0.31	78	0.27
2.0	0.36	91	0.77
4.0	0.34	87	0.47
10.0	0.26	65	0.36

REFERENCES

1. Dzhabiev, T.S. and Shilov, A.E., *Russ. Chem. Rev.*, 2012, vol. 81, no. 12, p. 1146. https://doi.org/10.1070/RC2012v081n
2. Kärkäs, M.D., Verho, O., Johnston, E.V., and Âkermark, B., *Chem. Rev.*, 2014, vol. 114, p. 11863. https://doi.org/10.1021/cr400572
3. Sartorel, A., Bonchio, M., Campagna, S., and Scandola, F., *Chem. Soc. Rev.*, 2013, vol. 42, p. 2262.
4. Geletii, Y.V., Huang, Zh., Hou, Yu., et al., *J. Am. Chem. Soc.*, 2009, vol. 131, p. 7522. https://doi.org/10.1021/ja901373m
5. Umena, Y., Kawakami, K., Shen, Y.R., and Kamiya, M., *Nature*, 2011, vol. 473, p. 55. https://doi.org/10.1038/nature09913
6. Hurst, J.K., *Science*, 2010, vol. 328, p. 315. https://doi.org/10.1126/science.1187721
7. Gersten, S.W., Samuels, G.J., and Meyer, T.J., *J. Am. Chem. Soc.*, 1982, vol. 104, p. 4029. https://doi.org/10.1021/ja00378a053
8. Yagi, M. and Kaneko, M., *Chem. Rev.*, 2001, vol. 101, p. 21. https://doi.org/10.1021/cr9801081
9. Sens, C., Romero, I., Rodriguez, M., et al., *J. Am. Chem. Soc.*, 2004, vol. 126, p. 7798. https://doi.org/10.1021/ja0486824
10. Suess-Fink, G., *Angew. Chem., Int. Ed. Engl.*, 2008, vol. 47, p. 5888. https://doi.org/10.1002/anie.200801121
11. Sartorel, A., Carraro, M., Scorrano, G., et al., *J. Am. Chem. Soc.*, 2008, vol. 130, p. 5006. https://doi.org/10.1021/ja0778371
12. Geletii, Y.V., Botar, B., Koegerler, P., et al., *Angew. Chem. Int. Ed. Engl.*, 2008, vol. 47, p. 3896. https://doi.org/10.1002/anie.200705652
13. Dzhabieva, Z.M., Shilov, G.V., Tkachenko, V.Yu., Avdeeva, L.V., and Dzhabiev, T.S., *Russ. J. Inorg. Chem.*, 2016, vol. 61, no. 6. p. 688. https://doi.org/10.1134/S003602361606005X
14. Dzhabieva, Z.M., Tkachenko, V.Yu., and Dzhabiev, T.S., *High Energy Chem.*, 2017, vol. 51, no 3, p. 215. https://doi.org/10.1134/S0018143917030043
15. Tkachenko, V.Yu., Dzhabieva, Z.M., Shilov, G.V., Avdeeva, L.V., Dobrygin, V.V., and Dzhabiev, T.S., *Russ. J. Inorg. Chem.*, 2021, vol. 66, no. 3, p. 354. https://doi.org/10.31857/S0044457X21030181
16. Hatchard, C.G. and Parker, C.A., *Proc. R. Soc. London: Ser. A*, 1956, vol. 235, no. 1203, p. 518.
17. Terenin, A.N., *Fotonika molekul krasitelei i rodstvennykh organicheskikh soedinenii* (Photonics of Dyes and Related Organic Compounds), Leningrad: Nauka, 1967.

Translated by S. Zatonsky